Cross-Layer Analysis of Scheduling Gains: Application to LMMSE receivers in Frequency-Selective Rayleigh-Fading Channels

R. Combes*, S.E. Elayoubi * and Z. Altman*
* Orange Labs, 38/40 rue du Général Leclerc, 92794 Issy-les-Moulineaux
Email:{richard.combes,salaheddine.elayoubi,zwi.altman}@orange-ftgroup.com

Abstract

This paper proposes two novel contributions: a fast statistical method for scheduling gain calculation is introduced, and we show how it can be combined with queuing theory and real network measurements in order to calculate the flow-level performance of a cellular network that uses Proportional Fair (PF) scheduling. A statistical method to evaluate the scheduling gain is proposed and a proof of its convergence is given. This method is three orders of magnitude faster than full system simulation. Based on these results, a queuing theory analysis is performed and is applied to the pedestrian A 3km/h channel model and LMMSE receiver. The evaluation uses drive tests measurements to reflect the realistic distribution of radio conditions. The derived flow-level performance of PF scheduling, including blocking rate, outage rate and flow throughput, is of major interest for network operators.

Index Terms

mobile networks, PF scheduler, LMMSE receiver, frequency selective Rayleigh fading channels.

I. Introduction

In recent years, there has been an important amount of research on how to evaluate the performance of the packet schedulers in Beyond 3G and 4G wireless networks. The evaluation at the system level is already non-trivial as the performance depends on physical layer characteristics such as the fading model or the receiver type. Flow-level performance analysis is even more challenging since it introduces another time scale corresponding to arrivals and departure of calls. Note that, by flow level performance, we mean the user-perceived QoS including blocking rates, outage rates and user throughput, taking into account the dynamics of arrivals and departures in the network.

In this paper we propose a fast statistical method based on kernel density estimation to evaluate scheduling gains for realistic physical layer models. We make use of the framework introduced in [1] for scheduling gain calculation and extend it for a general receiver and channel model. We then show the impact of scheduling on the flow-level performance of the network for elastic traffic and show how measurements can be incorporated in the model.

A flow-level performance analysis for elastic traffic in mobile networks was considered in [2]. In the paper [3], Bonald and Proutière showed the capacity gain resulting from channel-aware scheduling can be incorporated in flow level capacity analysis. The approach was extended in [4] to a more general channel model and the stability of PF scheduling was analyzed. A matched filter bound for PF scheduling on frequency-selective Rayleigh-fading channels was given in [5]. From a physical layer perspective, the link level performance of the LMMSE on a wide-band system in a macro-cell environment was addressed in several previous contributions, for example in [6]. To the best of our knowledge, none of the previous contributions has incorporated PF scheduling in a Frequency-Selective Rayleigh-Fading Channel and studied it from a flow level perspective.

The contributions of this paper are as follows:

- A statistical method to evaluate the scheduling gain is proposed and a proof of its convergence is given. The method is valid for any channel model and receiver type and is three orders of magnitude faster than a full system simulation.
- A queuing theory analysis of the performance of PF scheduling for elastic traffic for any channel model and receiver using the proposed method is developed, and is applied to the pedestrian A 3km/h model and LMMSE receiver.

- A demonstration of how measurement results from drive tests and realistic channel models can be used for network dimensioning and performance evaluation given the PF scheduling is shown.

The paper is organized as follows: Section II shows the statistical method used to calculate the scheduling gain and a convergence proof is given. The channel and receiver model are introduced in Section III and the scheduling gains for a static population of users are analyzed, using drive test measurements for the radio conditions. Section IV introduces the queuing model used for the evaluation of the flow-level performance and the impact of the network scheduling is demonstrated. Section V concludes the paper.

II. PF SCHEDULING AND SCHEDULING GAIN CALCULATION

A. PF scheduling

Let us consider N_u users, with $(t_n)_{n\in\mathbb{N}}$ - a set of scheduling instants, S_{i,t_m} - the instantaneous SINR of user i at time t_m and $r_{i,t_m} = \Phi(S_{i,t_m})$ - the corresponding instantaneous bitrate with Φ being a quality table for the AWGN channel obtained by link-level simulations. We define $S_i = \mathbb{E}[S_{i,t_m}]$ the mean SINR of user i which we assume to be stationary. We consider the PF scheduler which chooses user $i^*_{t_m} = \arg\max_i(\frac{S_{i,t_m}}{S_i})$ for transmission at time t_m, and we denote by $\overline{r}_i$ the mean throughput allocated to user i by such a scheduler. We then have ([1]):

$$\overline{r}_i = \int_0^{+\infty} \Phi(S_i x) \left[\prod_{j\neq i} F_j(x)\right] p_i(x)dx \tag{1}$$

where p_i is the probability distribution function (p.d.f) of $\frac{S_{i,t_m}}{S_i}$ and $F_i(x) = \int_0^x p_i(y)dy$ its cumulative distribution function (c.d.f). We define the scheduling gain as the ratio between the PF scheduler throughput and the throughput obtained with a Round Robin(RR) scheduler.

B. Estimation of SINR density

For a general receiver and channel model, neither p_i or F_j are available in closed form and we show here a statistical technique which enables us to estimate them from samples of the instantaneous SINR. We assume that we are able to obtain these samples by simulating the considered channel model and receiver. It is noted that while obtaining a c.d.f from samples is usually straightforward by considering the empirical c.d.f, estimating a p.d.f is usually notably more difficult, especially if the underlying p.d.f is multi-modal or does not exhibit good regularity properties. For example [7] shows that it is impossible to construct a p.d.f estimator which is unbiased, even if asymptotically unbiased estimators exist. To estimate the p.d.f we make use of an estimation method known as Kernel Density Estimation (KDE), introduced by Rosenblatt and Parzen [7], [8]. We consider a sample of i.i.d variables $(X_{k,i})_{k\geq 0}$ distributed according to $p_i(x)$. To estimate $F_i(x)$ we consider the empirical c.d.f:

$$\hat{F}_i^{(n)}(x) = \sum_{k=1}^{n} \mathbf{1}_{\{X_{k,i}\leq x\}} \tag{2}$$

We consider a function $K : \mathbb{R} \to \mathbb{R}^+$, with $K(-u) = K(u), u \in \mathbb{R}$, $\int_{-\infty}^{+\infty} K(u)du = 1$ known as the kernel. This gives rise to the following estimator for $p_i(x)$:

$$\hat{p_i}^{(n)}(x) = \frac{1}{nh(n)} \sum_{k=1}^{n} K\left(\frac{x - X_{k,i}}{h(n)}\right) \tag{3}$$

where $h(n)$ is a parameter known as the bandwidth which decreases when n grows. For subsequent numerical applications, we choose a Gaussian kernel: $K(u) = \frac{e^{-\frac{u^2}{2}}}{\sqrt{2\pi}}$. A natural estimator for the scheduling throughput in (1) is:

$$\hat{r}_i^{(n)} = \int_0^{+\infty} \Phi(S_i x) \left[\prod_{j\neq i} \hat{F}_i^{(n)}(x)\right] \hat{p_i}^{(n)}(x)dx \tag{4}$$

We will now prove that our estimate converges in mean square, using the following assumptions:

Assumptions. (i) $h(n)$ is non increasing, $h(n) \to 0$ and $nh(n) \to +\infty$
(ii) $p_i(x)$, $p_i'(x)$, $\Phi(S_i x)^2 p_i(x)$ are integrable on $\mathbb{R}^+$
(iii) There exists $\alpha > 0$ so that $x^{2\alpha} p_i(x)^2$ and $\frac{\Phi(S_i x)^2}{x^{2\alpha}}$ are integrable on $\mathbb{R}^+$ and $|x|^{2\alpha} K(x)$ is integrable on $\mathbb{R}$

Those assumptions require $p_i(x)$ to vanish rapidly when $x \to +\infty$ and to be reasonably regular, and Φ to be slowly increasing. A case of interest is $\Phi(x) = \log_2(1+x)$ since it corresponds to the Shannon capacity formula. For example, if we have $h(n) = n^{-\frac{1}{2}}$, $p_i(x) \underset{x \to +\infty}{\sim} e^{-ax}$, $a > 0$, $\Phi(x) = \log_2(1+x)$ and K a Gaussian kernel then the assumptions above hold.

We will need the following lemma:

Lemma 1. *Under our assumptions:* $\int_0^{+\infty} x^{2\alpha} \mathbb{E}[(\hat{p_i}^{(n)}(x) - p_i(x))^2] dx \underset{n \to +\infty}{\to} 0$

Proof: See appendix. ■

The convergence of the estimate is then given by the following theorem;

Theorem 1. *Under our assumptions we have that* $\mathbb{E}[(\hat{r}_i^{(n)} - \overline{r}_i)^2] \underset{n \to \infty}{\to} 0$

Proof: See appendix. ■

III. Link-level model

A. Channel Model

For the frequency-selective Rayleigh-fading channel, the channel impulse response $h(t)$ is:

$$h(t) = \sum_{l=1}^{L} h_l \delta(t - \tau_l) \tag{5}$$

with τ_l is the delay of the l-th tap, h_l - a circular-symmetric complex normal variable. Furthermore $\mathbb{E}[h_l] = 0$, $\mathbb{E}[h_l^* h_l] = \overline{h_l^2}$ the mean power of the l-th tap, and $\mathbb{E}[h_l^* h_{l'}] = 0$, $l \neq l'$. $(\overline{h_l^2}, \tau_l)_{1 \leq l \leq L}$ are given by the channel model we are considering. In this work we choose the Pedestrian A 3km/h model (see table I) that is a good representation of the channel in urban dense areas [9].

Pedestrian A 3km/h	
Relative delay (ns)	Relative mean power (dB)
0	0
110	-9.7
190	-19.2
410	-22.8

TABLE I
Pedestrian A 3km/h

B. LMMSE receiver

We consider an HSDPA system where mobiles are equipped by the LMMSE receiver, which is the most used receiver in Beyond 3G systems since it restores partially the inter-code orthogonality which is destroyed by the frequency selective channel. Given a channel realization $(h_l)_{1 \leq l \leq L}$ we can then use the results of [6] to obtain a closed-form for the Signal to Interference plus Noise Ratio (SINR). We thus introduce the channel matrix:

$$H = \begin{bmatrix} h_{L-1} & \cdots & h_0 & 0 & \cdots & 0 \\ 0 & h_{L-1} & \cdots & h_0 & & \vdots \\ \vdots & & \ddots & & \ddots & 0 \\ 0 & \cdots & 0 & h_{L-1} & \cdots & h_0 \end{bmatrix} \tag{6}$$

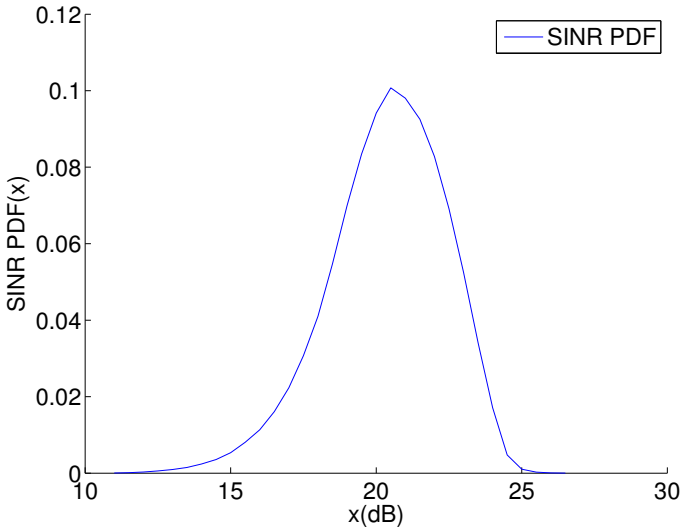

Fig. 1. distribution of the average SINR over the cell.

we obtain the SINR:

$$SINR = \frac{|g_0|^2 \frac{E_s}{N_0}}{\frac{c}{N}\sum_{i=-q-L+1, i\neq 0}^{q} |g_i|^2 \frac{E_s}{N_0} + \sum_{i=-q}^{q} |f_i|^2} \tag{7}$$

with E_s the symbol energy, $E_c = \frac{E_s}{N}$, N the spreading factor, N_0 the thermal noise, $q > 0$ with $2q+1$ the number of taps of the LMMSE filter, H_{q+L} - the $q+L$-th column of H, c - the number of codes used. The impact of the LMMSE receiver is given by the functions:

$$f = (HH^* + \frac{N_0}{E_c} I)^{-1} H_{q+L} \qquad \text{and} \qquad g = f^* H \tag{8}$$

C. Results

In order to evaluate the gains of the PF scheduler in a realistic setting, we consider real network drive test measurements. The measurement campaign has been run in the center of a major European town. Measurements are available for hundreds of cells, and one typical cell is selected for the capacity calculations (measurement samples are filtered with the scrambling code of the selected cell). This cell is composed of several (non contiguous) parts, which is common in live networks, especially in urban areas, because of irregular propagation from both the serving cell and the many interfering cells around, and because of the irregular cell planning. 1000 measurement samples are available for this cell. The average CPICH(Common PIlot CHannel) Ec/I0 on the cell is -7db, and the average CPICH RSCP (Received Signal Code Power) is -65dBm. The map of the drive test is shown in Figure 2.

We thus obtain the p.d.f of the average SINR over the cell, shown in Figure 1. In order to obtain the scheduling gain for different user configurations, we consider a number of users in the cell that goes from 1 to 10, and whose average SINRs are distributed following the drive test results. For simplicity, we discretize the p.d.f. into C different radio conditions, each of which is associated to a different average SINR. The state of the system is thus described by $\mathbf{s} = (n_1, ..., n_C)$, where n_c is the number of users of radio conditions c. Figures 3 and 4 show the c.d.f and the p.d.f respectively of the instantaneous SINR (normalized by the mean SINR) estimated by the method described above for two different "positions" in the cell, corresponding to the cell edge and cell center users. It is noted that we only represent two positions for clarity and that the subsequent capacity calculations involve all radio conditions. We can see that the two distributions are clearly different, most notably the distribution for cell edge users exhibits a lighter tail. This is important because the diversity gain is larger if the p.d.f of the instantaneous SINR has a heavy tail, since with a PF scheduler users transmit when they have the best normalized SINR. This figure demonstrates that the impact of the LMMSE receiver is non-negligible, since if we only consider a matched-filter bound all users have the same normalized SINR p.d.f. Figure 5 shows the scheduling gain for cell center and cell edge users. As expected, the gain increases rapidly with the number of users, and begins saturating when the number of users

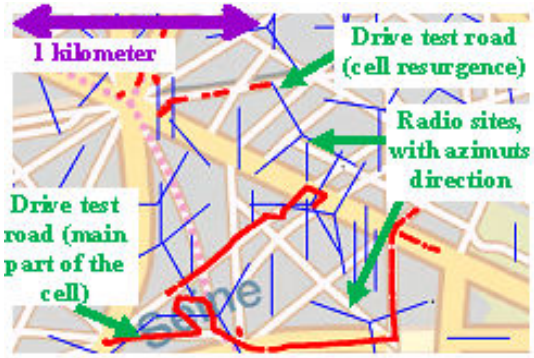

Fig. 2. Map of the drive test for the measured cell.

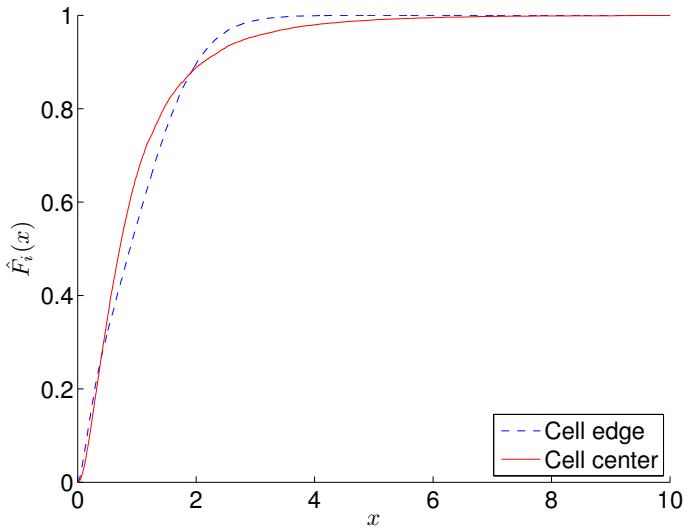

Fig. 3. Estimation of the instantaneous SINR c.d.f for different positions in the cell.

becomes large. On the other hand, the gain is larger at low SINR as cell center users are already close to the maximal throughput. An important observation is that this gain fluctuates around an average value, depending on the positions of other users in the cell. This is a new result in PF scheduling as, in flat Rayleigh channels, the PF scheduling gain depends only on the average SINR of the user and not on the radio conditions of other users [1]. However this fluctuation is not very large and we will see, in the flow level capacity analysis section, that the PF scheduling gain can be considered as equal to its trend.

D. Advantage of the proposed method

The advantage of the proposed method over full simulation of the system is that once the p.d.fs have been estimated, the mean throughput calculation is very fast, the difference being about three orders of magnitude. This is essential since the flow level evaluation requires a large number of evaluations of the users' throughput, making the full simulation method inapplicable. Furthermore, the extension of the method for max throughput and max-min fair schedulers is straightforward.

We now give an estimate of the speedup factor with respect to full system simulation. For each vector $\mathbf{n} \in \mathbb{N}^C$, $\sum_{i=1}^{C} n_i \leq N_{max}$, we have to calculate the scheduling gain. We call $\mathcal{N}_{config} = \{\mathbf{n} \in \mathbb{N}^C | \sum_{i=1}^{C} n_i \leq N_{max}\}$ the set of all possible configurations, and $N_{config} = \sum_{\mathbf{n} \in \mathcal{N}_{config}} \sum_{i=1}^{C} n_i$ the sum of the number of users on this set. In a full system simulation, for each configuration, we have to simulate $\sum_{i=1}^{C} n_i$ times the channel for N_{slots}. It is noted that a channel simulation corresponds to the inversion of $HH^* + \frac{N_0}{E_c} I$, which is a Toeplitz matrix of size $2q+1$.

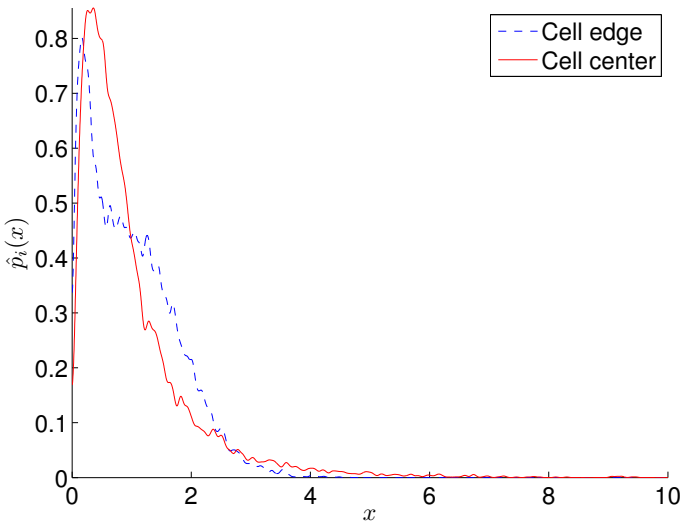

Fig. 4. Estimation of the instantaneous SINR p.d.f for different positions in the cell.

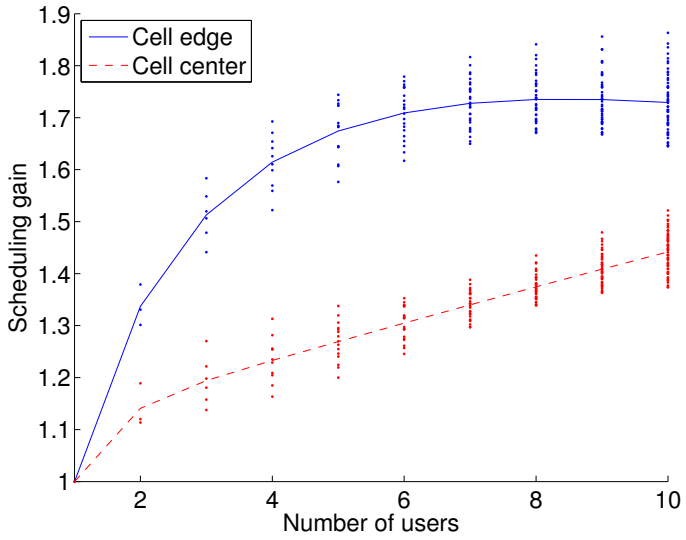

Fig. 5. Scheduling gains at different positions in the cell.

Using the Levinson-Durbin algorithm the inversion can be done in quadratic time $O((2q+1)^2)$. In the proposed method, for each radio condition we have to simulate the channel N_{pdf} times to estimate the corresponding p.d.f's. Once the p.d.fs have been estimated, the scheduling gain is obtained by a one-dimensional numerical integration using equation (4), which amounts to $O(N_{grid}\sum_{i=1}^{C} n_i)$ with N_{grid} the size of the grid used for the numerical integration. The system simulation amounts to $O(N_{slots}(2q+1)^2 N_{config})$, while the new method amounts to $O(CN_{pdf}(2q+1)^2 + N_{grid}N_{config})$. We have that N_{config} increases exponentially with C, hence $N_{grid}N_{config}$ dominates $N_{pdf}(2q+1)^2$ when the number of radio conditions C grows large. A rough estimate of the performance gain, ignoring the possibly large constants in the complexity analysis is $\frac{N_{slots}(2q+1)^2 N_{config}}{N_{grid}N_{config}} = 5.10^3$ with typical values: $N_{slots} = 1000$, $(2q+1)^2 = 1000$, $N_{grid} = 200$. This justifies the claim of 3 orders of magnitude gain.

IV. Flow-level capacity analysis

In the previous section, we studied the PF throughput gains at the different positions within a cell, for different numbers of users. To analyze the impact of PF scheduling on network performance and account for the users arrivals and departures, a flow-level capacity analysis is required.

A. Markovian analysis

When considering an elastic traffic, the heterogeneity in radio conditions translates into a larger service time for cell edge users. The service rate becomes state-dependent and the elements of the transition matrix $\mathbf{Q}$, indicating the transitions between states $\mathbf{s} = (n_1, ..., n_C)$ and $\mathbf{s}' = (n'_1, ..., n'_C)$, within the state space $\mathcal{S}$, are given by:

$$q(\mathbf{s}, \mathbf{s}') = \begin{cases} \lambda_c & n'_c = n_c + 1 \\ \frac{n_c D_c G_c(\mathbf{s})}{F \sum_{i=1}^{C} n_i} & n'_c = n_c - 1 \end{cases} \tag{9}$$

where λ_c is the arrival rate of users of radio condition c, F is the average file size, and D_c is the stand-alone throughput (i.e. the throughput obtained when the there is only one user in the cell having radio condition c). $G_c(\mathbf{s})$ is the scheduling gain for users of radio conditions c when the state of the system is described by $\mathbf{s}$, calculated as in the previous section.

The system is Markovian if the arrival rates are Poisson and the file size is exponentially distributed [10]. Let $\mathbf{\Pi}$ be the vector of steady-state probabilities $\pi(\mathbf{s})$, $\mathbf{s} \in \tilde{\mathcal{S}}$. These steady-state probabilities are obtained by solving the set of equations:

$$\mathbf{\Pi Q} = \mathbf{0} \tag{10}$$

with a normalization to 1 of these probabilities. The QoS is related here to the throughput received by users: A target throughput is fixed and a large proportion of users (say 90%) must achieve this target.

B. Processor sharing analysis

If we consider, from Figure 5, the average gain in each region of the cell when there are n users in the cell $G_c(n)$, the cell can be modeled as a Generalized Processor Sharing queue, and its evolution described by the overall number of users in a cell $n = \sum_{c=1}^{C} n_c$. The solution of (10) has the simple form [3]

$$\pi(\mathbf{s}) = \frac{1}{\Gamma} \frac{n!}{\prod_{c=1}^{C} n_c!} \prod_{c=1}^{C} \frac{\rho_c^{n_c}}{\prod_{i=1}^{n_c} G_c(i)} \tag{11}$$

where $\rho = \lambda_c F / D_c$ and Γ is a normalizing constant. If a target throughput T is sought, the probability for users of radio condition c to achieve this throughput is given by:

$$QoS_c = \sum_{m=1}^{K_c} \pi[m] \tag{12}$$

where K_c is the maximal allowable number of users in the cell such that the throughput of a user in position c is acceptable, calculated by:

$$K_c = \arg\min_{k_c} \frac{D_c G_c(k_c)}{k_c} - T \tag{13}$$

under the constraint $\frac{D_c G_c(k_c)}{k_c} \geq T$.

The overall QoS is given by:

$$\bar{QoS} = \sum_{c=1}^{C} \frac{\lambda_c}{\lambda} QoS_c \tag{14}$$

Similarly, other QoS metrics such as file transfer time and blocking rate can be calculated.

C. Flow level capacity results

Figures 6 7 and 8 give the outage rate, blocking rate and flow throughput respectively when the traffic increases for the PF scheduler compared with the Round Robin case. By outage rate, we mean the probability that the throughput achieved by the user is less than the target throughput of 500 Kbps. We denote by "RR" the Round Robin case, "PF markov" the case in which we calculate the performance by the exact Markovian analysis (solving equation (10)) and "PF" the case in which we use a Processor Sharing analysis with the approximation that the PF gain depends only on the overall number of users in the cell. We can see on the three figures that this approximation

is valid when we are interested in the flow level capacity of the cell since the curves “PF markov” and “PF” are very close.

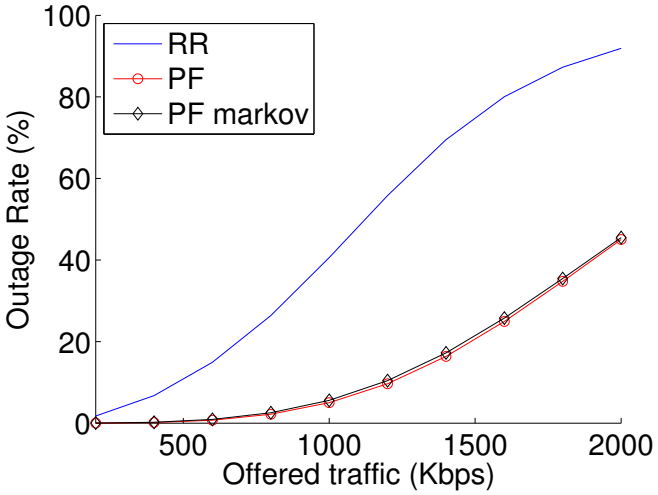

Fig. 6. Outage rate for Round Robin versus PF scheduling.

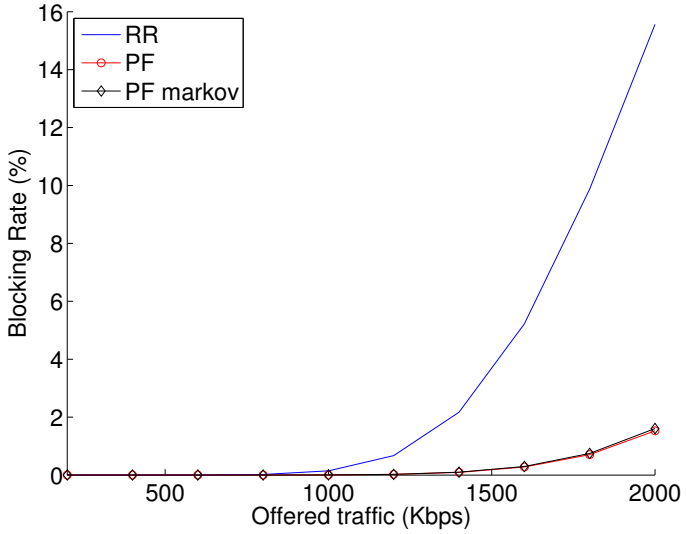

Fig. 7. Blocking rate for Round Robin versus PF scheduling.

As of the capacity gain, if a target of 10% outage is sought (90% of users are above 500 Kbps), we obtain a large capacity gain equal to 140%.

V. Conclusion

This paper has presented a cross-layer approach for estimating the PF scheduling gain and its impact on the network performance. The scheduling performance has been calculated using a fast statistical technique which is applicable to any channel model and receiver, and its convergence has been demonstrated. We have shown that this can be combined with a queuing analysis to calculate the flow-level performance of the network. To the best of our knowledge, this is the first work that calculates the flow level capacity (which is the capacity measure of interest for the operators), considering PF scheduling, LMMSE receivers and frequency-selective Rayleigh fading channels. Finally, using the results above, we have shown how to make use of network measurements to evaluate flow-level performance given PF scheduling with realistic propagation conditions.

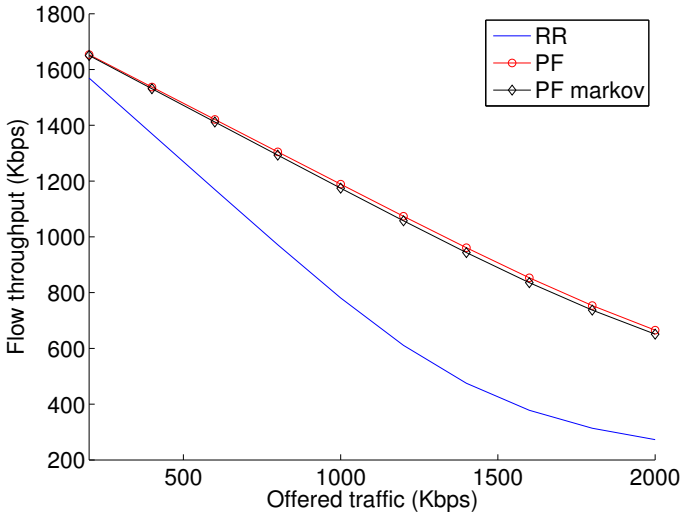

Fig. 8. Flow throughput for Round Robin versus PF scheduling.

APPENDIX A
PROOF OF LEMMA 1

Proof: We first show that $\sup_n \int_{A_\epsilon}^{+\infty} x^{2\alpha}\mathbb{E}[(\hat{p_i}^{(n)}(x) - p_i(x))^2]dx \underset{A_\epsilon \to +\infty}{\to} 0$, in order to get rid of the error due to the tail of $\hat{p_i}$. Using the convention $p_i(x) = 0$, $x < 0$, let $A_\epsilon > 0$:

$$\begin{aligned}
&\int_{A_\epsilon}^{+\infty} x^{2\alpha}\mathbb{E}[(\hat{p_i}^{(n)}(x) - p_i(x))^2]dx \\
&= \int_{A_\epsilon}^{+\infty} x^{2\alpha}\left(\int_{-\infty}^{+\infty} K(u)[p_i(x - h(n)u) - p_i(x)]du\right)^2 dx \\
&\leq \int_{-\infty}^{+\infty} K(u)\left(\int_{A_\epsilon}^{+\infty} x^{2\alpha}[p_i(x - h(n)u) - p_i(x)]^2 dx\right)du \\
&\leq \int_{-\infty}^{+\infty} K(u)\left(\int_{A_\epsilon}^{+\infty} x^{2\alpha}[p_i(x - h(n)u)^2 + p_i(x)^2]dx\right)du \qquad (15)
\end{aligned}$$

The expression in (15) is now separated in two terms. The first term gives:

$$\begin{aligned}
&\int_{-\infty}^{+\infty} K(u)\left(\int_{A_\epsilon}^{+\infty} x^{2\alpha}p_i(x)^2 dx\right)du \\
&= \int_{A_\epsilon}^{+\infty} x^{2\alpha}p_i(x)^2 dx \underset{A_\epsilon \to +\infty}{\to} 0 \qquad (16)
\end{aligned}$$

We make the change of variables $x \to x + h(n)u$ and use the convexity of $x \to x^{2\alpha}$ to apply the Jensen inequality to the second term:

$$\begin{aligned}
&\int_{-\infty}^{+\infty} K(u)\left(\int_{A_\epsilon}^{+\infty} x^{2\alpha}p_i(x - h(n)u)^2 dx\right)du \\
&\leq 2^{2\alpha-1}\left[\left(\int_{-\infty}^{+\infty} K(u)\left(\int_{A_\epsilon - |u|h(0)}^{+\infty} x^{2\alpha}p_i(x)^2 dx\right)du\right)\right. \\
&\left.+h(0)^{2\alpha}\left(\int_{-\infty}^{+\infty} K(u)|u|^{2\alpha}\left(\int_{A_\epsilon - |u|h(0)}^{+\infty} p_i(x)^2 dx\right)du\right)\right] \qquad (17)
\end{aligned}$$

Hence $\sup_n \int_{A_\epsilon}^{+\infty} x^{2\alpha}\mathbb{E}[(\hat{p_i}^{(n)}(x) - p_i(x))^2]dx \underset{A_\epsilon \to +\infty}{\to} 0$ by dominated convergence. We can now truncate the error in two terms. Let A_ϵ so that $\int_{A_\epsilon}^{+\infty} x^{2\alpha}\mathbb{E}[(\hat{p_i}^{(n)}(x) - p_i(x))^2]dx \leq \epsilon$, $\forall n$. We can use the result of [11](Page 1817,

Equation (10)), since $nh(n) \to +\infty$, and $p_i(x)$, $p_i'(x)$ are both square integrable, which gives:

$$\begin{aligned}&\int_0^{A_\epsilon} x^{2\alpha}\mathbb{E}[(\hat{p_i}^{(n)}(x) - p_i(x))^2]dx \\ &\leq A_\epsilon^{2\alpha}\int_0^{A_\epsilon} \mathbb{E}[(\hat{p_i}^{(n)}(x) - p_i(x))^2]dx \underset{n\to+\infty}{\to} 0\end{aligned} \tag{18}$$

Hence for all $\epsilon > 0$, we can find (A_ϵ, n_0) so that $\int_0^{+\infty} x^{2\alpha}\mathbb{E}[(\hat{p_i}^{(n)}(x) - p_i(x))^2]dx \leq 2\epsilon$, $n \geq n_0$ which concludes our demonstration. ■

APPENDIX B
PROOF OF THEOREM 1

Proof: We decompose the error in two terms, one linked to the estimation error of the c.d.f and the other to the estimation error of the p.d.f:

$$\begin{aligned}&\overline{r}_i - \hat{r}_i^{(n)} \\ &= \int_0^{+\infty} \Phi(S_i x)\left[\left(p_i(x) - \hat{p_i}^{(n)}(x)\right)\prod_{j\neq i}\hat{F}_j^{(n)}(x)\right. \\ &+ \left.\left(\prod_{j\neq i}F_j^{(n)}(x) - \prod_{j\neq i}\hat{F}_j^{(n)}(x)\right)p_i(x)\right]dx \\ &= A + B\end{aligned} \tag{19}$$

With:

$$A = \int_0^{+\infty} \Phi(S_i x)\left(p_i(x) - \hat{p_i}^{(n)}(x)\right)\prod_{j\neq i}\hat{F}_j^{(n)}(x)dx$$

$$B = \int_0^{+\infty} \Phi(S_i x)\left(\prod_{j\neq i}F_j^{(n)}(x) - \prod_{j\neq i}\hat{F}_j^{(n)}(x)\right)p_i(x)dx$$

Let $\alpha > 0$ satisfying our assumptions, we apply the Cauchy-Schwartz inequality to the first term:

$$\begin{aligned}\mathbb{E}[A^2] \leq &\left[\int_0^{+\infty}\left[\frac{\Phi(S_i x)}{x^\alpha}\right]^2 dx\right] \\ &\left[\int_0^{+\infty} x^{2\alpha}\mathbb{E}[(\hat{p_i}^{(n)}(x) - p_i(x))^2 dx\right]\end{aligned} \tag{20}$$

and $\mathbb{E}\left[A^2\right] \underset{n\to\infty}{\to} 0$ using lemma 1. Using the Jensen inequality on the second term we obtain:

$$B^2 \leq \int_0^{+\infty} \Phi(S_i x)^2\left[\prod_{j\neq i}F_j^{(n)}(x) - \prod_{j\neq i}\hat{F}_j^{(n)}(x)\right]^2 p_i(x)dx \tag{21}$$

Because of independence, and that $\mathbb{E}[\hat{F}_j^{(n)}(x)] = \hat{F}_j(x)$, $\forall j$, we have that $\mathbb{E}[\prod_{j\neq i}\hat{F}_j^{(n)}(x)] = \prod_{j\neq i}F_j^{(n)}(x)$, and $\mathbf{Var}(F_j^{(n)}(x)) = \frac{F_j(x)(1-F_j(x))}{n} \leq \frac{1}{n}$.

Hence $\mathbb{E}\left[\left(\prod_{j\neq i}F_j^{(n)}(x) - \prod_{j\neq i}\hat{F}_j^{(n)}(x)\right)^2\right] \leq 2\frac{N_u}{n}$.

Finally:

$$\mathbb{E}\left[B^2\right] \leq 2\frac{N_u}{n}\int_0^{+\infty}\Phi(S_i x)^2 p_i(x)dx \tag{22}$$

therefore $\mathbb{E}\left[B^2\right] \underset{n\to\infty}{\to} 0$ and $\mathbb{E}[(\hat{r}_i^{(n)} - \overline{r}_i)^2] \underset{n\to\infty}{\to} 0$ which completes the proof. ■

REFERENCES

[1] R. Combes, Z. Altman, and E. Altman, "On the use of packet scheduling in self-optimization processes: application to coverage-capacity optimization," in *WiOpt 2010*, Avignon, France, Jun. 2010.

[2] E.Altman, "Capacity of multi-service cellular networks with transmission-rate control: a queueing analysis," in *ACM Mobicom*, 2002, pp. 205–214.

[3] T. Bonald and A. Proutière, "Wireless downlink data channels: User performance and cell dimensioning," in *ACM Mobicom*, 2003.

[4] S. Borst, "User-level performance of channel-aware scheduling algorithms in wireless data networks," *IEEE/ACM Trans. Netw.*, vol. 13, pp. 636–647, June 2005.

[5] R. Combes, Z. Altman, and E. Altman, "Scheduling gain for frequency-selective rayleigh-fading channels with application to self-organizing packet scheduling," *Performance Evaluation: WiOpt 2010 special issue*, 2011.

[6] A. Saadani and J. B. Landre, "Realistic performance of HSDPA evolution 64-QAM in macro-cell environment," in *Vehicular Technology Conference, 2009. VTC Spring 2009. IEEE 69th*, Barcelona, 2009, pp. 1–5.

[7] M. Rosenblatt, "Remarks on some nonparametric estimates of a density function," *Annals of Mathematical Statistics*, vol. 27, pp. 832–837, 1956.

[8] E. Parzen, "On estimation of a probability density function and mode," *Annals of Mathematical Statistics*, vol. 33, pp. 1065–1076, 1962.

[9] K. L. H. Asplund and P. Okvist, "How typical is the "typical urban" channel model? mobile-based delay spread and orthogonality measurements," in *IEEE VTC spring*, 2008.

[10] N. Hegde and E. Altman, "Capacity of multiservice wcdma networks with variable gos," *Wireless Networks (Springer)*, vol. 12, pp. 241–253, 2006.

[11] M. R. Rosenblatt, "Curve estimates," *Annals Of Mathematical Statistics*, vol. 42, pp. 1815–1842, 1971.